Although bulk CE mixtures are good models for interpreting the equilibrium thermodynamic properties of cellular CE-rich inclusions, the present study has shown that heterogeneous nucleation of undercooled, fluid lipid occurs with bulk mixtures; hence, these mixtures are poor models for studying the kinetic properties of the phase behavior of cellular inclusions. CE dispersions consisting of microdroplets with approximately the same average diameter as that of the cellular inclusions constitute a more appropriate model for predicting the time dependence of the cellular lipid phase changes because homogeneous nucleation occurs. The present study suggests that in cells at 37 °C CP within inclusions containing up to 50% CP should be liquid crystalline (or liquid) under steady-state conditions.

ACKNOWLEDGMENTS

We express our gratitude to Dr. John F. Brandts (University of Massachusetts, Amherst) for his generous offer to use the facilities at MicroCal, Inc. (Northampton, MA), for several of our experiments. We also thank his engineer, Sam Williston, for his assistance.

Registry No. Cholesteryl oleate, 303-43-5; cholesteryl palmitate, 601-34-3.

REFERENCES

Adelman, S. J., Glick, J. M., Phillips, M. C., & Rothblat, G. H. (1984) *J. Biol. Chem. 259*, 13844–13850.
Becker, R., & Doring, W. (1935) *Ann. Phys. 24*, 719–731.
Brown, M. S., & Goldstein, J. L. (1983) *Annu. Rev. Biochem. 52*, 223–261.
Brown, M. S., Ho, Y. K., & Goldstein, J. L. (1980) *J. Biol. Chem. 255*, 9344–9352.
Carroll, R. M., & Rudel, L. L. (1981) *J. Lipid Res. 22*, 359–363.
Eyring, H., & Eyring, E. M. (1963) *Modern Chemical Kinetics*, Reinhold Publishing Co., New York.
Ginsburg, G. S., Atkinson, D., & Small, D. M. (1984) *Prog. Lipid Res. 23*, 135–167.
Glick, J. M., Adelman, S. J., Phillips, M. C., & Rothblat, G. H. (1983) *J. Biol. Chem. 258*, 13425–13430.
Katz, S. S., & Small, D. M. (1980) *J. Biol. Chem. 255*, 9753–9759.
Lundberg, B. (1985) *Atherosclerosis (Shannon, Irel.) 56*, 93–110.
Mims, M. P., Guyton, J. R., & Morrisett, J. P. (1986) *Biochemistry 25*, 474–483.
Oliver, M. J., & Calvert, P. P. (1975) *J. Cryst. Growth 30*, 343–351.
Phipps, L. W. (1964) *Trans. Faraday Soc. 60*, 1873–1883.
Rothblat, G. H., Rosen, J. M., Insull, W., Jr., Yau, A. O., & Small, D. M. (1977) *Exp. Mol. Pathol. 26*, 318–324.
Skoda, W., & Van den Tempel, M. (1963) *J. Colloid Sci. 18*, 568–584.
Small, D. M. (1986) *Handb. Lipid Res. 4*, 395–473.
Small, D. M., & Shipley, G. G. (1974) *Science (Washington, D.C.) 185*, 222–229.
Snow, J. W., McCloskey, H. M., Glick, J. M., Rothblat, G. H., & Phillips, M. C. (1988) *Biochemistry 27*, 3640–3646.
Turnbull, D. (1952) *J. Chem. Phys. 20*, 411–424.
Turnbull, D., & Fisher, J. C. (1949) *J. Chem. Phys. 17*, 71–73.
Volmer, M., & Weber, A. (1926) *Z. Phys. Chem. 119*, 277–301.
Wolfbauer, G. J. M., Minor, L. K., & Rothblat, G. H. (1986) *Proc. Natl. Acad. Acad. Sci. U.S.A. 83*, 7760–7764.

Localization of α1→3-Linked Mannoses in the N-Linked Oligosaccharides of *Saccharomyces cerevisiae mnn* Mutants†

Eugenio Alvarado, Lun Ballou, Luis M. Hernandez,‡ and Clinton E. Ballou*
Department of Biochemistry, University of California, Berkeley, California 94720
Received September 13, 1989; Revised Manuscript Received October 31, 1989

ABSTRACT: Neutral and phosphorylated N-linked oligosaccharides were isolated from *Saccharomyces cerevisiae mnn9* and *mnn9 gls1* mutant mannoproteins and separated into homologues that differed in the number of terminal α1→3-linked mannoses. In each type of oligosaccharide, the addition of such mannose was shown to occur in an ordered rather than a random fashion. The results confirm and extend an earlier report that dealt with the N-linked oligosaccharides from yeast invertase [Trimble, R. B., & Atkinson, P. H. (1986) *J. Biol. Chem. 261*, 9815–9824], and they suggest that the postulated processing pathway can be generalized to include phosphorylated and glucose-containing N-linked oligomannosides. We conclude that this processing pathway is identical for the analogous oligosaccharides from the *mnn9* and wild-type strains of *S. cerevisiae*. Analysis of the *mnn2 mnn10* mannoprotein revealed that a similar modification occurred at the branched terminus of the outer chain as well as in the core in this mutant.

The *mnn9*[1] mutant of *Saccharomyces cerevisiae* is a glycosylation-defective strain that makes mannoproteins that lack most of the outer chain portion of N-linked oligosaccharides (Ballou et al., 1980; Tsai et al., 1984a,b). A second glycosylation-defective mutant, called *mnn1*, lacks terminal α1→3-linked mannoses on both O- and N-linked oligosaccharides and on both the core and outer chain of the latter (Antalis et al., 1973; Raschke et al., 1973). The double mutant, *mnn1*

† This work was supported in part by National Science Foundation Grant PCM87-03141 and National Institutes of Health Grant AI-12522.
* To whom correspondence should be addressed.
‡ Visiting scholar from the Department of Microbiology, University of Extremadura, Badajoz, Spain.

[1] Abbreviations: M or Man, mannose; GlcNAc, *N*-acetylglucosamine; HOHAHA, homonuclear Hartmann–Hahn spectroscopy; ROESY, rotating-frame Overhauser enhancement spectroscopy; *mnn*, yeast mutant defective in protein glycosylation; H-1, H-2, and H-3, sugar ring protons, not to be confused with ^1H, ^2H, and ^3H; HPLC, high-performance liquid chromatography.

0006-2960/90/0429-2471$02.50/0

mnn9, makes asparagine-linked oligosaccharides with structure I (Hernandez et al., 1989a), whereas in the absence of the

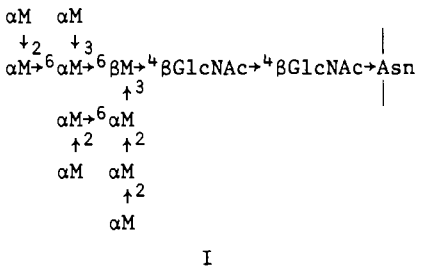

I

mnn1 defect several α1→3-linked mannose are added to the terminal mannose units of this structure. The objective of this study was to determine the locations of such mannose units.

Because the *Aspergillus satoi* exo-α1→2-mannosidase (Ichishima et al., 1981) is able to remove all of the terminal α1→2-linked mannose of the *mnn1 mnn9* core oligosaccharide (Tsai et al., 1984a,b) and because the removal of these mannoses leads to characteristic shifts in the anomeric proton NMR resonances of the remaining mannose units (Cohen & Ballou, 1980), a method is available to identify those α1→2-linked mannoses that are capped with α1→3-linked mannose (Trimble & Atkinson, 1986). Here we show that, in homologues of the neutral *mnn2 mnn9* oligosaccharides with 11–14 mannoses, the α1→3-linked mannoses are distributed in an ordered fashion between the terminal α1→2-linked mannoses. The same result was observed with the phosphorylated oligosaccharides and with the glucose-containing oligosaccharides that accumulate on mannoproteins in the *mnn2 mnn9 gls1* mutant (Tsai et al., 1984a,b) that is defective in glucosidase I (Saunier et al., 1982). These results confirm and extend the observations by Trimble and Atkinson (1986) for a series of oligosaccharides isolated from *S. cerevisiae* wild-type invertase, and they generalize the concept of an ordered pathway for the addition of α1→3-linked mannoses to the small N-linked oligosaccharides. A similar modification was observed on the terminus of the outer chain in the *mnn2 mnn10* mutant (Ballou et al., 1989).

Experimental Procedures

Materials and Methods. Oligosaccharides were obtained from the *mnn2 mnn9* (Ballou et al., 1980), *mnn2 mnn9 gls1* (Tsai et al., 1984a,b), and *mnn2 mnn10* (Ballou et al., 1989) mutants of *S. cerevisiae* X2180. The *mnn2* defect affects branching of the outer chain and has no recognized phenotype in the *mnn9* background whereas it is expressed in the *mnn10* background. The isolated mannoproteins were treated with endoglucosaminidase H and the released oligosaccharides were fractionated into homologues by gel filtration on a Bio-Gel P-4 column, while the phosphorylated oligosaccharide was purified by ion exchange on QAE-Sephadex (Hernandez et al., 1989b). The individual fractions were checked for homogeneity by HPLC on the Dionex BioLC carbohydrate system using the HPIC-AS6 (CarboPac PA1) column, which was eluted with a sodium acetate gradient in 100 mM NaOH. Methylation was done according to Ciucanu and Kerek (1984), and the reaction was processed according to Lindberg (1972). The sources of exo-α1→2-mannosidase (Ichishima et al., 1981), endo-α1→6-mannanase (Nakajima et al., 1976), gel filtration and ion exchange matrices, D_2O, and other reagents have been reported, as well as the methods for determination of carbohydrate and protein (Hernandez et al., 1989a).

The one-dimensional ^1H NMR spectra were done at 40 °C in D_2O on an AM-400 or AM-500 Bruker spectrometer in the Department of Chemistry on this campus (Cohen & Ballou, 1980; Vliegenthart et al., 1983; Derome, 1987). Acetone [δ 2.217 referenced to sodium 2-(trimethylsilyl)propanesulfonate] was the internal standard. The two-dimensional ^1H NMR spectra were recorded at room temperature in D_2O on the 400-MHz Bruker spectrometer equipped with a "reverse-mode" probe. The spectra were acquired in the phase-sensitive mode according to the time proportional phase incrementation method (Marion & Wüthrich, 1983). Data matrices of 1K × 512 points were accumulated with spectral widths of 950 Hz and relaxation delays of 1.5 s; 24 scans per FID were collected. Normal mode detection was employed, with the low-power output of the amplifier for the generation of all pulses and presaturation of the solvent with the decoupler. The homonuclear Hartmann–Hahn (HOHAHA) spectra were recorded with a mixing time of 125 ms, which allows the observation of only those crosspeaks due to short-range coherence transfer (Bax & Davis, 1985). The rf field strength for the spin lock was 6.5 KHz. After being zero-filled to 1K × 1K points, the data were multiplied in both dimensions by a sine-bell window function shifted by $\pi/2$. The rotating-frame Overhauser enhancement spectroscopy (ROESY) was adapted from Kessler et al. (1987). These experiments were recorded at a mixing time of 400 ms with an average rf field strength for spin locking of 650 Hz. The matrices were zero-filled to 4K × 4K points and multiplied in both dimensions by sine-bell window functions shifted by $\pi/8$ before the Fourier transformation. ROESY spectra were measured, instead of conventional NOESY spectra, because they provide stronger crosspeaks with the high molecular weight compounds under study.

Convention for Identifying Mannose Units in N-Linked Yeast Oligosaccharides. For convenience in specifying individual mannose units in yeast oligosaccharides, we have adopted the following convention (Hernandez et al., 1989b):

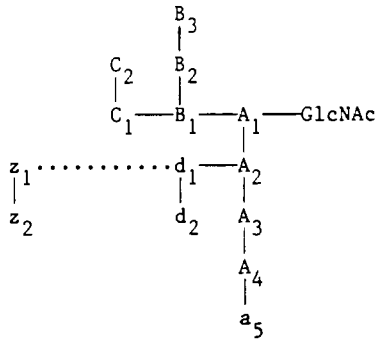

The letters stand for mannose units in which the horizontal bonds, with the exception of the linkage to GlcNAc, represent 1→6 linkages and the vertical ones are 1→2 and 1→3 linkages. Mannose units derived from the lipid-linked oligosaccharide precursor are shown in upper-case and those added during processing are shown in lower-case. The dotted line attached to d_1 indicates an extension of the 1→6-linked outer chain which is of variable length, and when the outer chain is elongated, d_2 is not present but an equivalent mannose (z_2) is added at the end (Ballou et al., 1989). Phosphorylation in the *mnn1 mnn9* mutant occurs on position 6 of mannoses C_1 and A_3, and in the *mnn1 mnn2 mnn10* mutant it occurs predominantly on z_1 and C_1 (Hernandez et al., 1989a,b; Ballou et al., 1989).

Results

Isolation of N-Linked Oligosaccharides from the mnn2 mnn9 Mutant. Mannoprotein was isolated from cells, grown to stationary phase on YEPD (1% yeast extract, 2% Bacto-

peptone, and 2% D-glucose), by autoclaving them in citrate buffer, pH 7.0, and the solubilized mannoprotein was precipitated with methanol, purified as the borate–Cetavlon complex, and fractionated on a DEAE-Sephacel column (Ballou et al., 1989). The major carbohydrate-containing fraction, eluted at 0.2 M NaCl, was digested with endoglucosaminidase H, and the released oligosaccharides were separated on a Bio-Gel P-4 column (2 × 190 cm) by elution with water in 1-mL fractions. The phosphorylated oligosaccharides were eluted first (peak A, fractions 120–150), followed by the neutral oligosaccharides (peak B, fractions 200–250). Peak B was divided in the middle into two parts and each was rerun on the Bio-Gel P-4 column in water. After several such steps, in which related fractions were recombined, four neutral oligosaccharides were obtained that appeared to differ from each other by one mannose and to consist of $Man_{11-14}GlcNAc$ on a column calibrated with $Man_{10}GlcNAc$. The peak tube of $Man_{11}GlcNAc$ was eluted at fraction 225, that of $Man_{12}GlcNAc$ at fraction 218, that of $Man_{13}GlcNAc$ at fraction 211, and that of $Man_{14}GlcNAc$ at fraction 204. The individual fractions were analyzed by HPLC on the Dionex BioLC system and gave the results in Figure 1. As shown, each contained small amounts of other homologues, and the chromatogram of a synthetic mixture of the four showed small peaks for isomeric products that were separated from the major peaks. Insufficient material was obtained to allow characterization of these minor components, but they could have biological importance.

Characterization of the Neutral Oligosaccharides. Although the use of anomeric proton (H-1) chemical shifts to make linkage assignments is empirical and has limitations, the approach is singularly applicable for structural determinations of the relatively simple high-mannose oligosaccharides and is based on a solid experimental foundation (Cohen & Ballou, 1980; Vliegenthart et al., 1983). The success of this application derives from the facts that the structural types are limited to α1→2-, α1→3-, and α1→6-linked mannose, which have very different chemical shifts of δ 5.03 ± 0.02, δ 5.13 ± 0.01, and δ 4.91 ± 0.01, respectively, and that substitution of such mannoses at position 2 deshields about 0.25 ppm while substitution at position 3 or 6 shields about 0.01 ppm, thereby leading to reproducible and characteristic changes. Some ambiguity arises in distinguishing between substitution of an α1→6-linked mannose at position 2 (δ 5.12 ± 0.005) and addition of an α1→3-linked mannose (δ 5.13 ± 0.01), but these changes can be differentiated because the first is accompanied by the loss of an H-1 signal at higher field whereas the second has minimal effect on the H-1 signal of the substituted mannose. The fact that mannose has an equatorial H-2 leads to sharper spectra and facilitates resolution of the H-1 signals. Finally, we have not relied solely on chemical shifts but have also employed two-dimensional homonuclear shift correlation spectroscopy when chemical shifts alone were insufficient for the purpose.

The H-1 NMR spectra of the four *mnn2 mnn9* oligosaccharides are shown in Figure 2 along with that of the $Man_{10}GlcNAc$ from the *mnn1 mnn9* mutant (Tsai et al., 1984a,b). All oligosaccharides show the 10 anomeric proton signals characteristic of the $Man_{10}GlcNAc$ structure (I), which suggests they have the same fundamental structure previously reported (Hernandez et al., 1989a), but in addition they have signals for 1–4 α1→3-linked mannoses that resonate at δ 5.12–5.14.

To locate the additional α1→3-linked mannoses, each oligosaccharide was digested with exo-α1→2-mannosidase, and

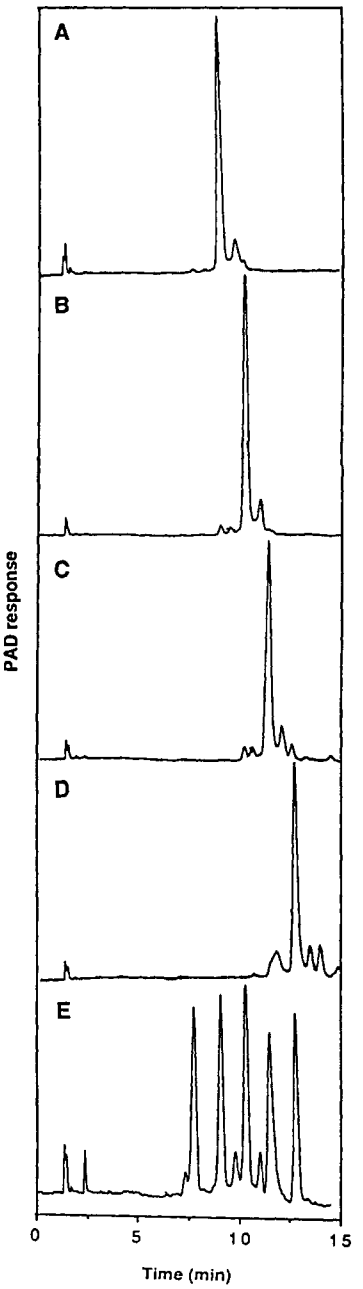

FIGURE 1: Comparison and separation of neutral oligosaccharides by HPLC. (A) $Man_{11}GlcNAc$ (20% of total); (B) $Man_{12}GlcNAc$ (35% of total); (C) $Man_{13}GlcNAc$ (35% of total); (D) $Man_{14}GlcNAc$ (10% of total). (E) Separation of a synthetic mixture of the four oligosaccharides plus $Man_{10}GlcNAc$, which was eluted at about 8 min. The Dionex BioLC system, fitted with a pulsed amperometric detector, was operated with a 30-min gradient of 50–200 mM sodium acetate in 100 mM NaOH.

the H-1 NMR spectrum of the recovered oligosaccharide was determined. The smallest homologue, $Man_{11}GlcNAc$ (Figure 2B), contained a single extra α1→3-linked mannose and yielded a product with two fewer mannoses on enzymic digestion. A reduction in the signal at δ 5.04 confirmed that two α1→2-linked mannoses (C_2 and d_2) were removed, and the spectrum (Figure 2C) revealed the appearance of two unsubstituted α1→6-linked mannoses at δ 4.90 (C_1) and 4.92 (d_1). The result is consistent only with structure II and indicates that the starting oligosaccharide had structure III, in which a single α1→3-linked mannose is attached to mannose A_4.

A single mannose was removed from the $Man_{12}GlcNAc$ (Figure 2D) by the exo-α1→2-mannosidase, and the product

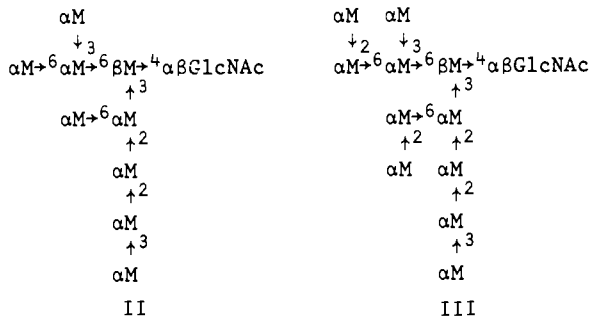

II III

(Figure 2E) showed a major new signal at δ 4.92 and a minor signal at δ 4.90. Since these chemical shifts correspond to unsubstituted α1→6-linked mannoses, the possible structures are IV and V. The assignment of structure IV to the major

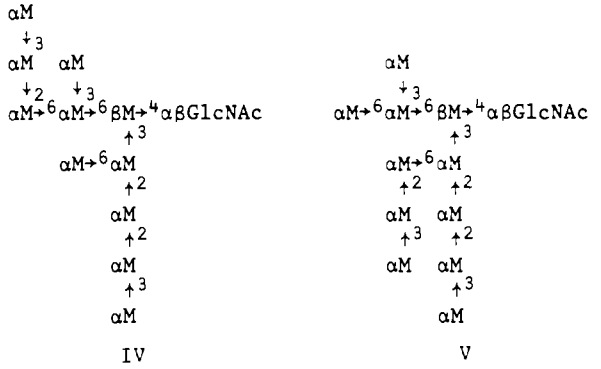

IV V

compound is supported by the strong signal at δ 4.92 (mannose d_1) and by the loss of the signal for mannose d_2 on the lower field side of the multiplet at δ 5.02–5.05. These results indicate that the original oligosaccharide was a 3:1 mixture of isomers with structures VI and VII.

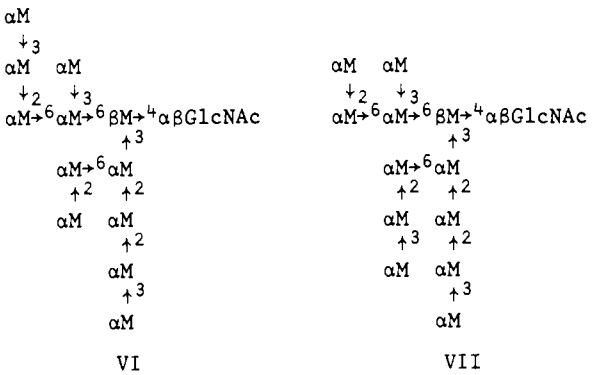

VI VII

Exo-α1→2-mannosidase digestion of the two larger oligosaccharides, $Man_{13}GlcNAc$ (Figure 2F) and $Man_{14}GlcNAc$ (Figure 2G), released only traces of mannose and left the compounds largely unchanged. Thus, $Man_{13}GlcNAc$ must have structure VIII, wheras $Man_{14}GlcNAc$ has structure VIII with a fourth α1→3-linked mannose in an unassigned position.

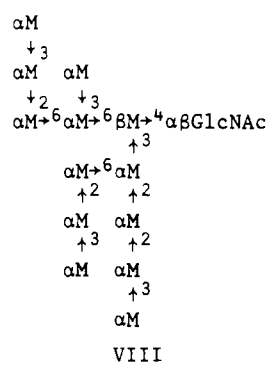

VIII

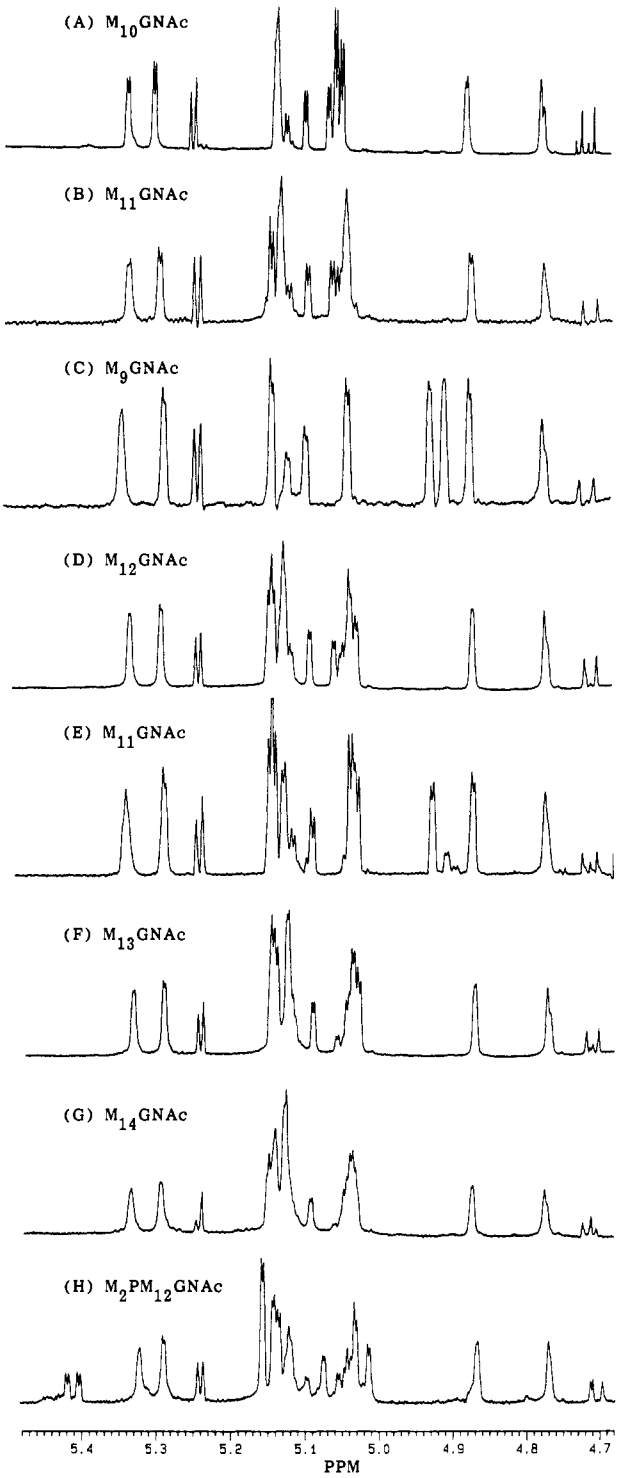

FIGURE 2: H-1 NMR spectra of the *mnn9* oligosaccharides. (A) $Man_{10}GlcNAc$ from the *mnn1 mnn9* mutant; (B–H) oligosaccharides from the *mnn2 mnn9* mutant; (B) $Man_{11}GlcNAc$; (C) $Man_9GlcNAc$ obtained by exo-α1→2-mannosidase digestion of (B); (D) $Man_{12}GlcNAc$; (E) $Man_{11}GlcNAc$ obtained by exo-α1→2-mannosidase digestion of (D); (F) $Man_{13}GlcNAc$; (G) $Man_{14}GlcNAc$; (H) Man_2P-$Man_{12}GlcNAc$. M is mannose; GNAc is *N*-acetylglucosamine.

Structural Assignment by Two-Dimensional ^1H NMR Spectroscopy. A problem in making positional assignments for the α1→3-linked mannose units is that they do not induce as significant a chemical shift on the anomeric (H-1) protons of the mannoses to which they are linked as is observed for α1→2 substitution (Cohen & Ballou, 1989). It was expected, however, that the H-3 protons of the substituted mannoses would experience a downfield shift relative to those of the

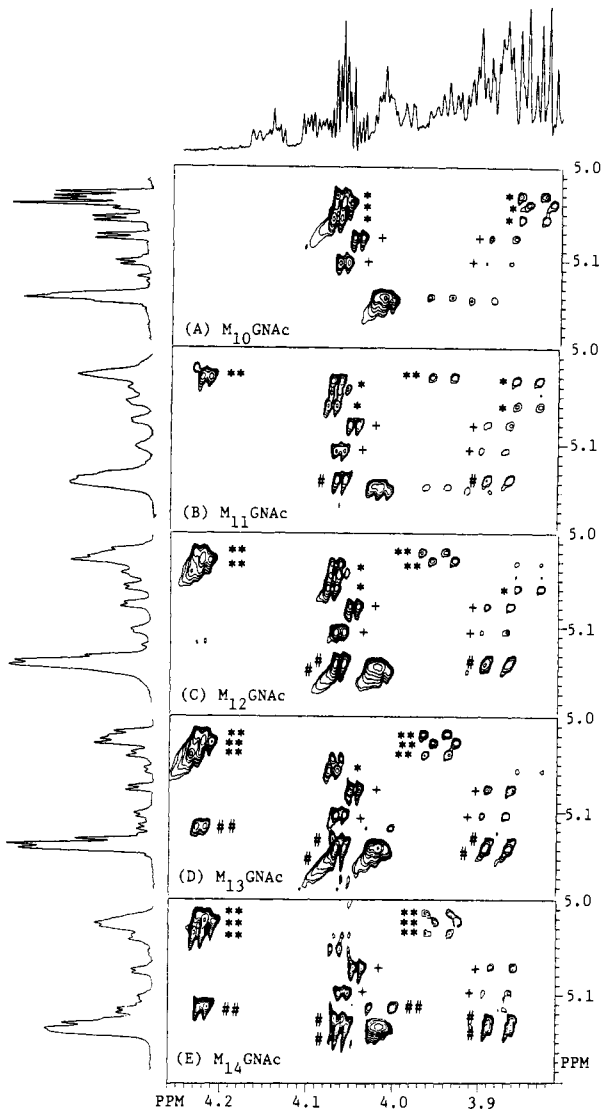

FIGURE 3: Partial HOHAHA spectra of the *mnn2 mnn9* oligosaccharides. H-2 signals appear at δ 4.0–4.1 and H-3 signals at δ 3.8–3.9, for unsubstituted α1→2-linked mannoses, and these are identified with single symbols. H-2 signals appear at δ 4.20–4.23 and H-3 signals at δ 3.92–3.97, after deshielding by 3-subsitution, and these are identified with double symbols. The H-2 and H-3 protons of mannoses A_4, C_2, and d_2 are indicated by (*), those of mannose B_2 by (+), and those of mannoses a_5, c_3, d_3, and d_4 by (#). The left spectra are for the anomeric protons, and the top spectrum is for the outer ring protons of the Man_{10}GlcNAc and does not show the changes associated with addition of α1→3-linked mannoses. M is mannose; GNAc is *N*-acetylglucosamine.

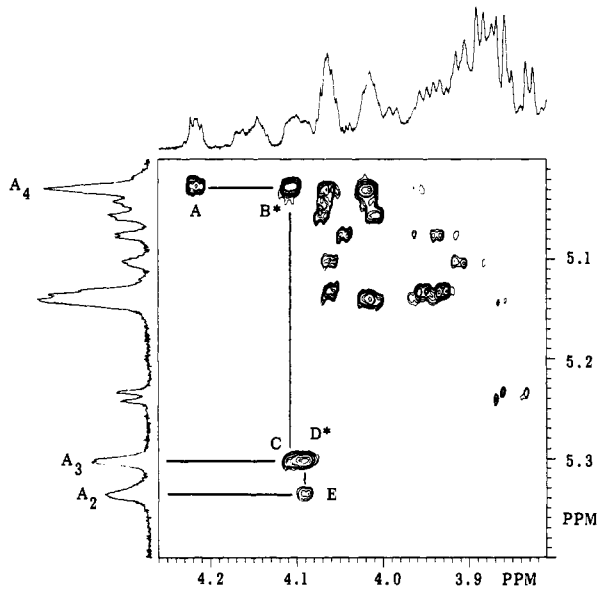

FIGURE 4: Partial ROESY spectrum of Man_{11}GlcNAc. This spectrum shows the connectivities between mannoses A_4, A_3, and A_2. The interresidue peak B* results from an NOE between H-1 of A_4 and H-2 of A_3, the intraresidue H1 and H2 peaks being A and C; the interresidue peak D* results from an NOE between H-1 of A_3 and H-2 of A_2, the intraresidue H-1 and H-2 peaks being C and E. This identifies H-2 of A_4 as the signal that is shifted downfield to δ 4.21 by substitution at position 3.

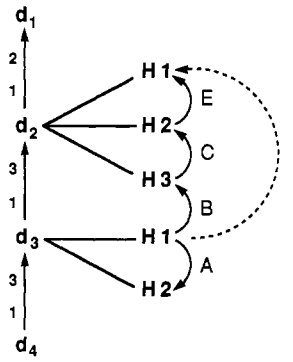

FIGURE 5: Diagram summarizing the NOEs measured to relate H-1 of d_3 to H-1 of d_2. The overall relation is indicated by the dashed arrow while the solid arrows show the stepwise relationships. H-1 of d_3 is identified by its intraresidue NOE with H-2, which is deshielded owing to substitution by d_4. H-1 of d_3 gives an interresidue NOE with H-3 of d_2, which shows an intraresidue NOE to H-2, whereas H-2 gives an intraresidue NOE with H-1. The letters A, B, C, and E refer to the panels of Figure 6 in which the actual two-dimensional contours are displayed.

unsubstituted mannoses in compound I. Because the one-dimensional spectra of these oligosaccharides are very crowded in the region corresponding to the ring protons, however, such spectra cannot provide unambiguous assignments of the H-3 protons of each terminal α1→2-linked mannose unit. These assignments were obtained with HOHAHA experiments (Bax & Davis, 1985) that provide direct correlations between the H-1, the chemical shifts of which are known with high confidence, and the H-2 and H-3 protons. To simplify the two-dimensional spectra, a mixing time in the pulse sequence was chosen so that only the H-1 to H-2 and the H-1 to H-3 correlations would be observed. As a complement, the ROESY spectra (Kessler et al., 1987) allow the sequencing of the mannose units in the side chains that have α1→2 and α1→3 linkages (Hernandez et al., (1989a).

Analyses of HOHAHA and ROESY spectra of the compounds confirm and extend the assignments made in the previous section. Substitution at position 3 of a mannose unit causes a downfield shift of its H-2 proton as well as its H-3 proton and leads to an NOE between H-1 of the substituent mannose and H-3 of the substituted mannose. By comparing the HOHAHA spectrum of Man_{10}GlcNAc, which lacks terminal α1→3-linked mannose (Figure 3A), with that of the Man_{11}GlcNAc, which has a single terminal α1→3-linked mannose (Figure 3B), we observe the downfield shift of a single H-2 proton from δ 4.065 to δ 4.220 that is correlated with an H-1 proton at δ 5.03. Although this is in a region where the H-1 signals for mannose A_4 and C_2 overlap, the shifted H-2 signal is clearly identified with mannose A_4 by the ROESY spectrum (Figure 4) in which interresidue crosspeaks can be traced from H-1 of mannose A_4 to H-1 of mannose A_3 (A→B*→C) and from H-1 of the latter to H-1 of mannose A_2 (C→D*→E). H-3 of mannose A_4 is also shifted downfield from δ 3.83 to δ 3.94. These results confirm structure III for

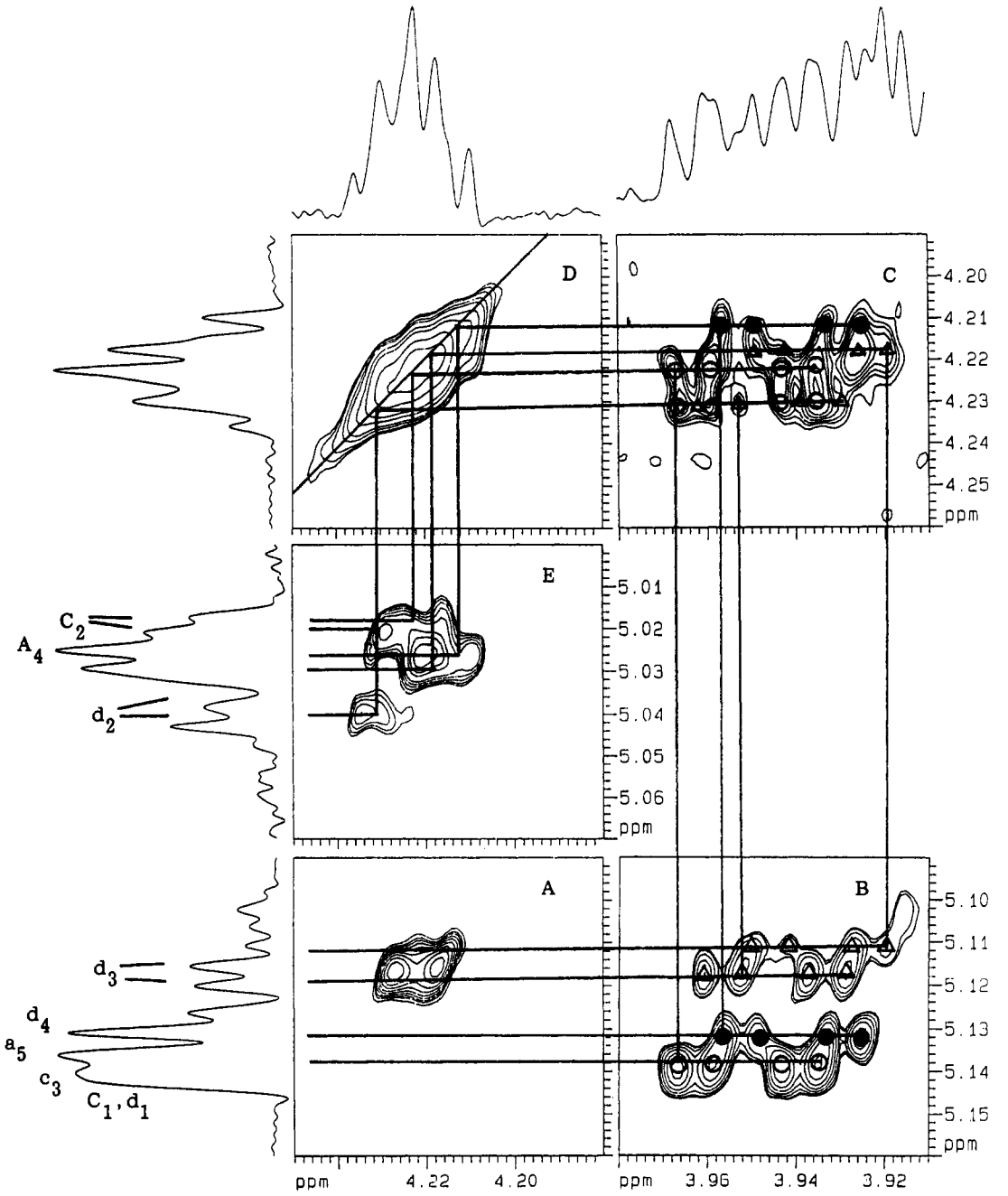

FIGURE 6: Composite partial ROESY spectrum of $Man_{14}GlcNAc$. The figure was constructed by juxtaposing enlarged sections of the ROESY spectrum that displayed intra- and interresidue crosspeaks for H-1, H-2, and H-3 of mannoses A_4, C_2, and d_2 with mannoses a_5, c_3, and d_3. Figure 5 illustrates the origin of the crosspeaks and how H-1 of d_3 can be indirectly correlated with H-1 of d_2 (dashed arrows). (A) H-1/H-2 crosspeak for the mannose (a_5, c_3, or d_3) that is shifted downfield to δ 4.22 owing to substitution at position 3. (B) Interresidue NOE crosspeaks between H-1 of mannoses a_5, c_3, and d_3 and H-3 of mannoses A_4, C_2, and d_2. The patterns suggest four doublets of doublets, two of which are correlated with the split d_2 signals. (C) Intraresidue H-2/H-3 NOE crosspeaks for mannoses A_4, C_2, and d_2; (D) diagonal for the H-2 signals of the same mannoses. (E) Intraresidue H-1/H-2 crosspeaks for mannoses A_4, C_2, and d_2. In (B), the contour peaks are marked with symbols that emphasize the patterns, while in (C) the pattterns of (B) are repeated to give the best fit of the contours.

the $Man_{11}GlcNAc$. Note that H-1 of mannose A_4 shifts upfield about 0.01 ppm upon 3-substitution (compare spectra A and B of Figure 3), as expected (Cohen & Ballou, 1980).

Similar inspection of the HOHAHA spectrum of the $Man_{12}GlcNAc$ (Figure 3C) reveals that a second pair of H-2 and H-3 signals is shifted downfield, and these signals are correlated with an H-1 signal at δ 5.035 in Figure 3B that moves to δ 5.020 in Figure 3C. This H-1 is assigned to mannose C_2 by its chemical shift, which is different from that of d_2, the H-1 signal of which is distinguished by a characteristic splitting due to a long-range interaction with the *N*-acetylglucosamine anomers (Vliegenthart et al., 1983). The results are consistent with structure VI for this homologue.

Finally, the HOHAHA spectrum of the $Man_{13}GlcNAc$ (Figure 3D) shows that all three H-2 signals for the terminal $\alpha 1 \rightarrow 2$-linked mannoses (A_4, C_2, and d_2) are deshielded and appear at δ 4.22–4.24, while all three H-3 signals are shifted from the region δ 3.82–3.86 to δ 3.93–3.97. These results confirm that in this homologue all terminal $\alpha 1 \rightarrow 2$-linked mannoses are substituted at position 3 as shown in structure VIII. There is, however, evidence for some heterogeneity because a portion of the H-2 signal associated with mannose d_2 is not deshielded, while a portion of the H-2 signal of a terminal $\alpha 1 \rightarrow 3$-linked mannose is shifted downfield as expected if it were substituted at position 3 (Cohen & Ballou, 1980). From this, we conclude that the sample of

$Man_{13}GlcNAc$ contains a significant amount of an isomer that has the parent structure VI with an additional $\alpha 1 \rightarrow 3$-linked mannose attached to mannoses a_5 and/or c_3.

The fourth $\alpha 1 \rightarrow 3$-linked mannose in the $Man_{14}GlcNAc$ proved more difficult to locate because it is attached to another $\alpha 1 \rightarrow 3$-linked mannose with a similar chemical shift. It was expected, however, that the $\alpha 1 \rightarrow 3$-mannose that is substituted at position 3 would experience a deshielding of its H-2 and H-3 protons, thereby making it identifiable. The HOHAHA spectrum of this oligosaccharide (Figure 3E) shows that essentially all of the three H-2 signals for mannoses A_4, C_2, and d_2 are shifted downfield to δ 4.20–4.22, while a fourth H-2 signal that is correlated with an H-1 signal at δ 5.11 is similarly affected. This latter H-1 signal has the chemical shift expected for a 3-substituted $\alpha 1 \rightarrow 3$-linked mannose, owing to the shielding effect of such substitution (Cohen & Ballou, 1980). The identity of the substituted mannose as d_3 was made by tracing the interresidue NOE from H-1 of this mannose to H-1 of mannose d_2 as illustrated in Figure 5, which summarizes the path documented in Figure 6. Consult the legend for an explanation of Figure 5.

Panel A of Figure 6 shows the crosspeak corresponding to the H-1/H-2 intraresidue NOE for the $\alpha 1 \rightarrow 3$-linked mannose (d_3) that is substituted at position 3. The corresponding NOEs for the unsubstituted $\alpha 1 \rightarrow 3$-linked mannoses (a_5, c_3, d_4) appear at δ 4.06–4.07 (not shown). Panel B shows the interresidue NOEs between H-1 of mannoses a_5, c_3, and d_3 and H-3 of the $\alpha 1 \rightarrow 2$-linked mannoses A_4, C_2, and d_2 to which they are attached. Each anomeric proton correlates with four peaks corresponding to the doublet of doublets of the H-3 protons. Note that the broad H-1/H-2 contour in panel A correlates with the upper cluster of signals in panel B, indicating that the anomeric proton of this mannose is split into two signals at δ 5.112 and 5.116 by a long-range interaction with the *N*-acetylglucosamine (Vliegenthart et al., 1983). In panel C, the H-3/H-2 intraresidue NOEs for mannoses A_4, C_2, and d_2 are shown. These NOEs are possible because, for mannose units, the distance between the equatorial H-2 proton and the axial H-3 proton is small. All signals from panel B are accommodated in the contours of panel C, with the complication that the H-2 signal of mannose C_2 is also split in this compound. The overlap of crosspeaks in panel C produces some deformations of the contours, but nevertheless, each doublet of doublets in panel B can be unambiguously correlated with a similar doublet of doublets in panel C as indicated with the symbols connected by vertical lines. Panel D shows the H-2 diagonal contours and panel E the intraresidue H-1/H-2 NOEs for mannoses A_4, C_2, and d_2. The interconnectivities between H-1 of the mannose with the deshielded H-2 in panel A and the anomeric proton signals along the left of panel E were traced as shown on the figure, which indicates that this mannose is linked to d_2. Note that the large characteristic splitting of the H-1 signal of d_2 is also observed in its H-2 and H-3 protons as evidenced in panel C. From this analysis, it appears that a region of the molecule that includes H-1 of d_3 and H-3, H-2, and H-1 of d_2 is located in space close to the reducing-end *N*-acetylglucosamine. Although mannose B_2 is also $\alpha 1 \rightarrow 3$-linked and, therefore, a potential acceptor for the 14th mannose in the $Man_{14}GlcNAc$, the HOHAHA spectra in Figure 3 demonstrate that the chemical shifts of the H-2 and H-3 signals of this mannose are not affected in any of the homologues.

Structure of the Phosphorylated Oligosaccharide. Ion exchange on QAE-Sephadex of peak A from the endoglucosaminidase H digest of the mannoprotein yielded a major fraction that was eluted at 25 mM NaCl in the position of a diesterified monophosphate (Varki & Kornfeld, 1980; Hernandez et al., 1989b), and only a small amount of carbohydrate was eluted later at the position characteristic of an oligosaccharide with two charges, that is, a monoesterified monophosphate or diesterified diphosphate.

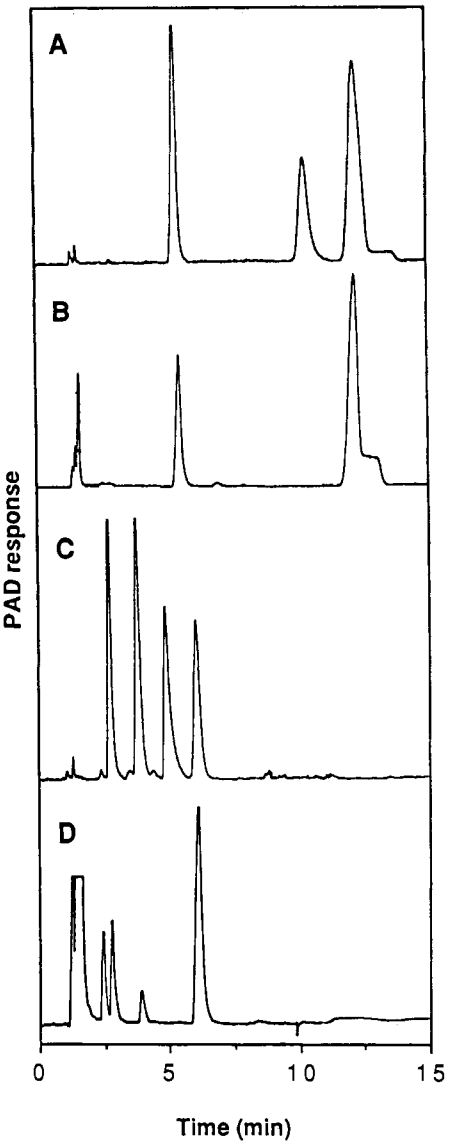

FIGURE 7: Characterization by HPLC of the products of mild acid hydrolysis of the phosphorylated oligosaccharide. (A) (Left to right) Standard mixture of mannose, $\alpha 1 \rightarrow 6$-mannobiose, and unresolved $\alpha 1 \rightarrow 2$- plus $\alpha 1 \rightarrow 3$-mannobiose; (B) products from acid hydrolysis of oligosaccharide phosphate; (C) (left to right), standard mixture of mannitol, $\alpha 1 \rightarrow 6$-mannobiitol, $\alpha 1 \rightarrow 2$-mannobiitol, and $\alpha 1 \rightarrow 3$-mannobiitol; (D) borohydride-reduced acid hydrolysis product which shows $\alpha 1 \rightarrow 3$-mannobiitol plus small amounts of mannitol and other products. The Dionex column was eluted with 75 mM NaOH for (A) and (B) and with 20 mM NaOH for (C) and (D). In both (B) and (D), the disaccharide product is eluted coincidently with the $\alpha 1 \rightarrow 3$ isomer. The peak preceding mannitol in (D) has the retention time of glucitol and probably resulted from isomerization of mannitol during the reduction.

The NMR spectrum of peak A, Figure 2H, gave a split H-1 signal at δ 5.41–5.43 that confirmed the presence of the mannosyl phosphate linkage, but it was shifted upfield by an amount to suggest that the mannose attached to the phosphate was substituted at position 3 by another mannose (Cohen & Ballou, 1980). This was established by mild acid hydrolysis of the glycosyl phosphate bond and characterization of the released sugar by HPLC on the Dionex BioLC carbohydrate system (Figure 7). Mannose and mannobiose were observed

in a molar ratio of 1:4 (Figure 7B). When the borohydride-reduced product was analyzed, it was eluted coincidently with mannitol and the reduced α1→3-mannobiose, the latter being separated from the reduced α1→2- and α1→6-mannobioses (Figure 7D). The NMR spectrum (Figure 2H) also shows a small signal at δ 5.43–5.45, about 20% of the total, for a mannosyl phosphate group, which suggests that this amount of the oligosaccharide had a single mannose linked to the phosphate group and accounts for the presence of mannose in the hydrolysate. Integration of the other H-1 signals in the spectrum indicated that the oligosaccharide had about 12 mannoses exclusive of those on the phosphate group. The spectrum was comparable to that of the $Man_{12}GlcNAc$ (Figure 2D), and exo-α1→2-mannosidase digestion removed a single mannose and gave a product with a spectrum that was similar to that of structure III. The slight shoulders on the signals at δ 4.87 and 5.32 and the small signal at δ 4.80 (Figure 2H) are characteristic of phosphorylation on mannose A_3; but this analogue appears to represent less than 5% of the preparation, with the major site of phosphorylation being mannose C_1 (Hernandez et al., 1989b).

The second component eluted from the QAE-Sephadex column gave a poorly resolved H-1 NMR spectrum (not shown) that was similar to that of the major peak, except that it lacked signals for the mannosyl phosphate group. This material, therefore, corresponds to the monoester form of the oligosaccharide and probably results from chemical hydrolysis of the diester during isolation of the mannoprotein (Hernandez et al., 1989b).

A portion of the phosphorylated oligosaccharide was dephosphorylated, and the neutral product was analyzed on the Dionex BioLC system. The pattern revealed four oligosaccharides with the same retention times as those shown in Figure 1, but with a preponderance of the $Man_{12}GlcNAc$ homologue. Thus, although it is clearly heterogeneous, the phosphorylated oligosaccharide fraction appears to be mainly the isomer with structure IX.

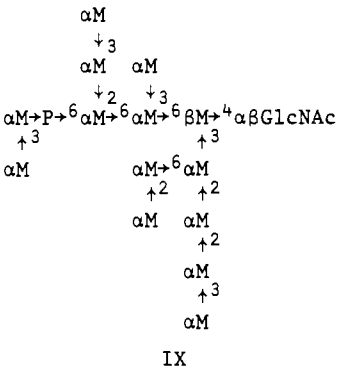

IX

Structure of the N-Linked Oligosaccharides from the mnn9 gls1 Mutant. This strain lacks the glucosidase I activity involved in removal of the three glucose units from the oligosaccharide precursor after its transfer to protein (Saunier et al., 1982). Consequently, one of the sites (mannose A_4) in the *mnn9* strain is unavailable for addition of an α1→3-linked mannose in the *mnn9 gls1* mutant (Tsai et al., 1984a,b). The oligosaccharide fraction obtained from the latter strain by endoglucosaminidase H digestion of the mannoprotein gave the H-1 NMR spectrum in Figure 8A, which suggested an average composition of $Glc_3Man_{11}GlcNAc$. Rather than fractionate this mixture, it was treated directly with exo-α1→2-mannosidase and then fractionated on a Bio-Gel P-4 column into three components. The one of smallest size was eluted at fraction 285, and the H-1 NMR spectrum (Figure 8B) indicated a composition of $Glc_3Man_8GlcNAc$. Removal of two α1→2-linked mannoses reduced the signal at δ 5.04 and exposed two α1→6-linked mannoses with H-1 signals at δ 4.90 (C_1) and 4.92 (d_1). Only a small fraction of a signal for an α1→3-linked mannose is seen at δ 5.14 and a single proton for a terminal α1→2-linked mannose at δ 5.04 (A_4). The results support structure X for this fragment.

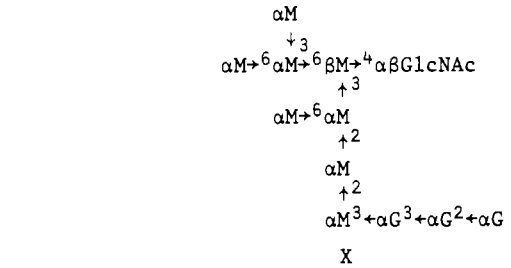

X

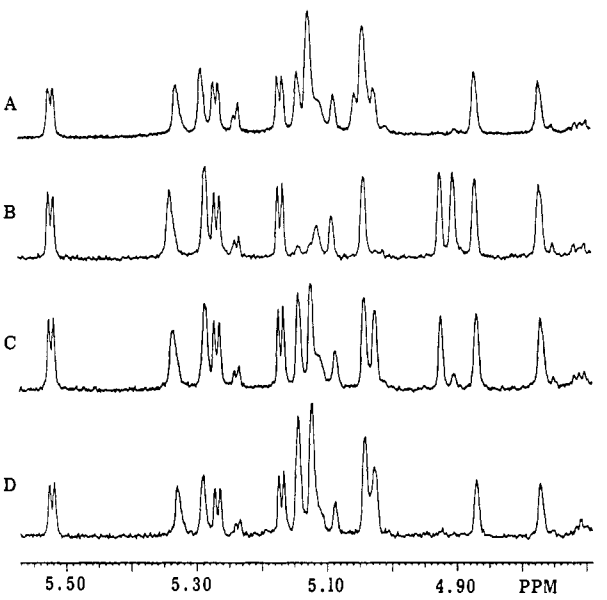

FIGURE 8: H-1 NMR spectra of the glucose-containing oligosaccharides. (A) Mixture of homologues before mannosidase digestion and separation by gel filtration; (B–D) Separated homologues produced by exo-α1→2-mannosidase digestion of (A); (B) $Glc_3Man_8GlcNAc$; (C) $Glc_3Man_{10}GlcNAc$; (D) $Glc_3Man_{12}GlcNAc$. (B) is derived from the homologue with no extra α1→3-linked mannose, while the precursor of (C) has one and the precursor of (D) has two such substituents. The H-1 signals of the three glucoses are recognizable at δ 5.17, 5.27, and 5.52 by their large splitting (Tsai et al., 1984a,b), similar to *N*-acetylglucosamine at δ 5.23.

A second oligosaccharide from the Bio-Gel P-4 column separation of the mannosidase digest gave the H-1 NMR spectrum in Figure 11C, which revealed a composition of $Glc_3Man_{10}GlcNAc$. A single signal for an α1→3-linked mannose is observed at δ 5.14, and two signals for terminal α1→2-linked mannoses are observed at δ 5.03 and 5.04. Removal of a single α1→2-linked mannose exposed the α1→6-linked mannose d_1 with an H-1 signal at δ 4.92. This result supports structure XI for the fragment.

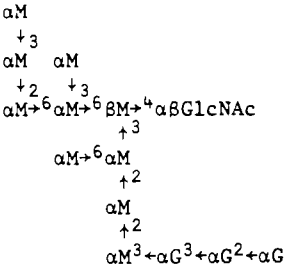

XI

The largest oligosaccharide from the Bio-Gel P-4 column, eluted at fraction 258, gave a spectrum (Figure 8D) that supported the composition $Glc_3Man_{12}GlcNAc$ and indicated the presence of two $\alpha 1 \rightarrow 3$-linked mannoses by integration of the signal at δ 5.14. The exo-$\alpha 1 \rightarrow 2$-mannosidase had no apparent effect on this oligosaccharide, from which we conclude that all terminal $\alpha 1 \rightarrow 2$-linked mannose is protected by substitution. Thus, the three oligosaccharides from the *mnn9 gls1* mutant must have structures XII–XIV.

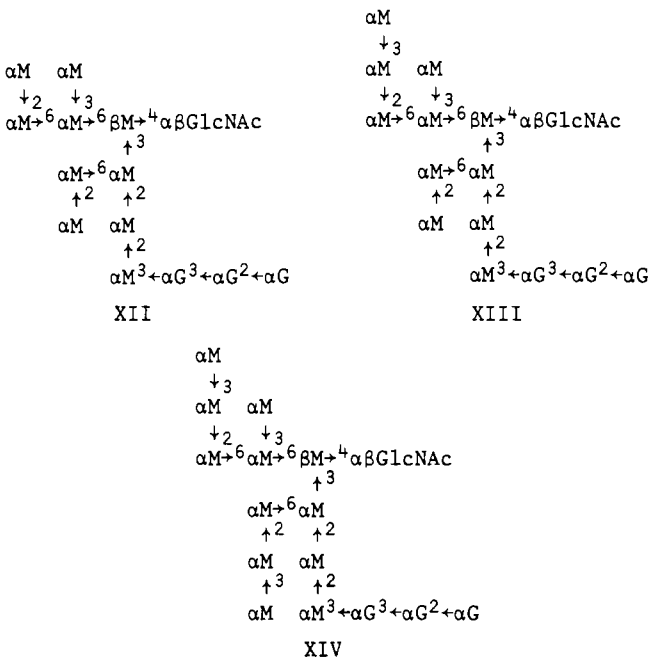

Structure of the N-Linked Oligosaccharide from the mnn2 mnn10 Mutant Mannoprotein. The endoglucosaminidase H released oligosaccharide fraction was eluted from a Bio-Gel P-4 column in a position similar to that obtained from the *mnn1 mnn2 mnn10* mutant (Ballou et al., 1989). The H-1 NMR spectrum of a fraction from the center of the peak (Figure 9A) was very similar to that of the *mnn1 mnn2 mnn10* oligosaccharide, except for the signal at δ 5.14 that is characteristic of an $\alpha 1 \rightarrow 3$-linked mannose unit. The integration suggested the presence of 1.5 such mannose units.

To determine the location of this $\alpha 1 \rightarrow 3$-linked mannose, the oligosaccharide was digested with a bacterial endo-$\alpha 1 \rightarrow$-6-mannanase (Nakajima & Ballou, 1974), which degrades the unbranched $\alpha 1 \rightarrow 6$-linked outer chain and yields a glucosamine-containing core fragment along with small fragments from the outer chain (Ballou et al., 1989). The digest was fractionated on a Bio-Gel P-4 column (Figure 10B), and the peaks were characterized by their H-1 NMR spectra (Figures 9 and 11). Peaks A and B (Figure 10B) were mannose and $\alpha 1 \rightarrow 6$-mannobiose, and peak C was identified by its NMR spectrum as $\alpha 1 \rightarrow 6$-mannotriose (Figure 11A). These come from the internal portion of the unbranched outer chain. A tetrasaccharide fragment (Figure 10B, peak D) and a pentasaccharide fragment (Figure 10B, peak E) were obtained that correspond in structure to the capped terminus of the outer chain (structures XV and XVI) (panels B and C of Figure 11).

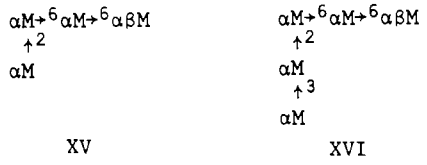

The ratios of these two fragments suggest that 70% of the capped outer chain termini are modified by the addition of an $\alpha 1 \rightarrow 3$-linked mannose unit. The structure assigned to XVI on the basis of its H-1 NMR spectrum was confirmed by methylation analysis, which yielded alditol acetates for 2,3,4,6-tetramethylmannose (1.3 mol), 2,4,6-trimethylmannose (1.2 mol), 3,4,6-trimethylmannose (1.0 mol), and 2,3,4-trimethylmannose (1.9 mol). The expected ratios were 1:1:1:2.

The core fragment was heterogeneous, but the spectrum of the peak tube of the major component H showed that it was a mixture of the two $Man_{10}GlcNAc$ isomers XVII and XVIII because the signal at δ 5.14, for a terminal $\alpha 1 \rightarrow 3$-linked mannose, and at δ 4.90, for an extra $\alpha 1 \rightarrow 6$-linked mannose, each integrated for about half of a mannose unit (Figure 9C). All other H-1 signals are also present in the $Man_9GlcNAc$

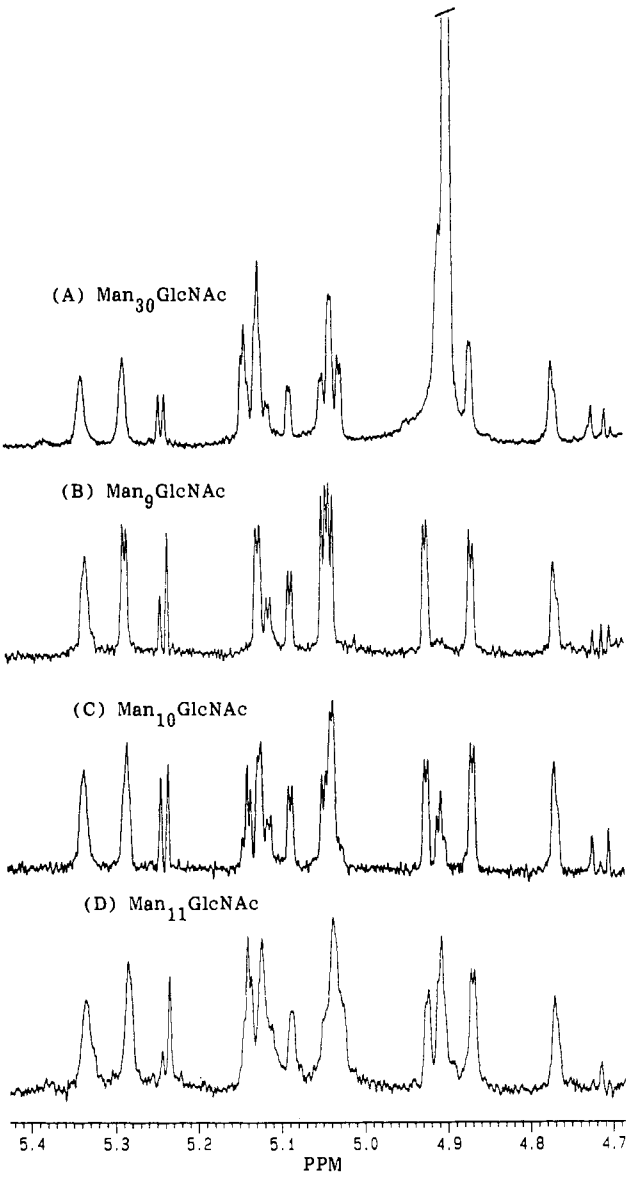

FIGURE 9: H-1 NMR spectra of *mnn10* oligosaccharides. (A) Intact *mnn2 mnn10* oligosaccharide, which has a signal at δ 5.14 for about one $\alpha 1 \rightarrow 3$-linked mannose that is absent in the *mnn1 mnn2 mnn10* oligosaccharide spectrum (Ballou et al., 1989); (B) peak G from Figure 10, whose spectrum agrees with a $Man_9GlcNAc$ consisting of the $Man_8GlcNAc$ precursor with attached $\alpha 1 \rightarrow 6$-linked mannose d_1; (C) peak H from Figure 10, whose spectrum is consistent with a $Man_{10}GlcNAc$ structure in which half of the molecules have two $\alpha 1 \rightarrow 6$-linked mannoses (signals at δ 4.90 and 4.92) and half have one $\alpha 1 \rightarrow 6$-linked (signal at δ 4.92) and one $\alpha 1 \rightarrow 3$-linked mannose (signal at δ 5.14); (D) peak I from Figure 10, whose spectrum is consistent with a $Man_{11}GlcNAc$ with two $\alpha 1 \rightarrow 6$-linked and one $\alpha 1 \rightarrow 3$-linked mannoses.

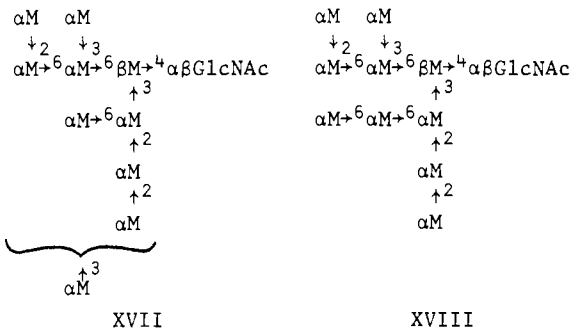

XVII XVIII

fragment G (Figure 9B), which was previously obtained by endomannanase digestion of the *mnn1 mnn2 mnn10* oligosaccharide (Ballou et al., 1989). The H-1 spectrum of peak I in Figure 10B showed that it combined both features of structures XVII and XVIII and had signals for one full proton at δ 4.90, 4.92, and 5.14 (Figure 9D). This indicates a composition of $Man_{11}GlcNAc$ with a single α1→3-linked mannose and two α1→6-linked mannoses. The broadened signal at δ 5.04 for α1→2-linked mannose and the splitting of the signal at δ 5.14 for α1→3-linked mannose suggest that this one mannose is distributed between mannoses A_4 and C_2.

Although the molar ratio between the oligosaccharides derived from the core and that from the capped terminus of the outer chain is a little greater than 1, the fragments support structure XIX, in which about two extra α1→3-linked mannose units are distributed equally between the starred positions in the core and the outer chain (XIX). Note that because mannose d_1 is not substituted at position 2 in the *mnn2 mnn10* strain (Ballou et al., 1989), addition of an α1→3-linked mannose at this position is precluded.

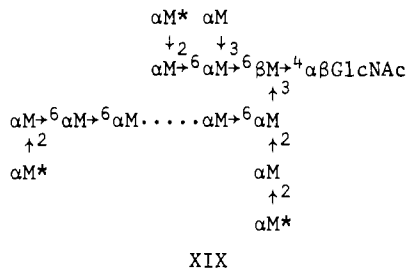

XIX

Discussion

In earlier studies from this laboratory on the asparagine-linked oligosaccharide fraction isolated from *S. cerevisiae mnn2* mutant mannoprotein by a combined digestion with endoglucosaminidase H and endo-α1→6-mannanase, it was observed that this "core" preparation was heterogeneous owing to variable amounts of terminal α1→3-linked mannose (Nakajima & Ballou, 1974; Cohen et al., 1982). Later it was found that this heterogeneity was absent in the core oligosaccharide from the *mnn1 mnn2* mutant (Cohen et al., 1982) owing to a defective α1→3-mannosyltransferase activity in the *mnn1* strain. Recently, Trimble and Atkinson (1986) have studied the localization of the terminal α1→3-linked mannose in the smallest N-linked oligosaccharides from bakers' yeast invertase with 11–14 mannoses, and their results suggested that these mannose units were added in a specific rather than a random order with increasing size of the homologues. We have applied a similar analysis of the neutral and phosphorylated N-linked oligosaccharides on mannoproteins from the *mnn2 mnn9* mutant and the neutral oligosaccharides from *mnn2 mnn9 gls1* and *mnn2 mnn10* mutants to obtain results that are consistent with those of Trimble and Atkinson (1986).

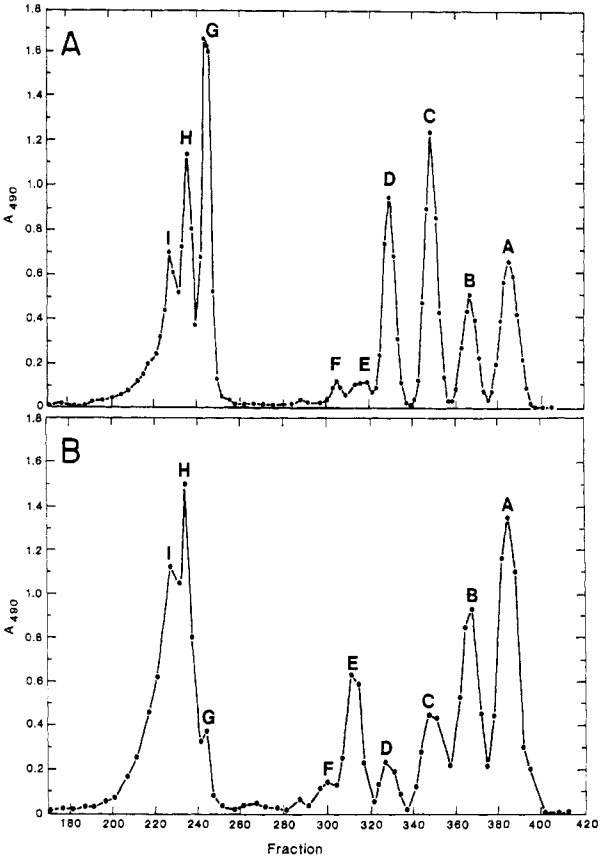

FIGURE 10: Gel filtration fractionation of the endo-α1→6-mannanase digest of *mnn2 mnn10* oligosaccharides. (A) *mnn1 mnn2 mnn10* oligosaccharide digest, taken from Ballou et al. (1989); (B) *mnn2 mnn10* oligosaccharide digest. Peaks A–F are mannose to mannohexaose, while peaks G–I are $Man_{9-11}GlcNAc$ homologues. In the absence of the *mnn1* mutation, peak E is increased at the expense of peak D, while peaks H and I are increased at the expense of peak G. These shifts are attributed to the addition of α1→3-linked mannoses.

The addition of terminal α1→3-linked mannose units to the *mnn2 mnn9* oligosaccharide $Man_{10}GlcNAc$ follows the preferred order A_4, C_2, d_2, according to the convention we have adopted, although there is some heterogeneity in the process. As expected, mannose A_4 is not affected in the glucosylated oligosaccharide in which it is already substituted, whereas the mannosyl phosphate group of the phosphorylated oligosaccharides is converted to an α1→3-mannobiosyl phosphate unit.

The phosphorylated *mnn2 mnn9* oligosaccharide fraction consisted almost exclusively of the monophosphate, whereas the diphosphate derivative is a major component in the *mnn1 mnn9* mannoprotein (Hernandez et al., 1989b). Because the mannosyl phosphate transferase that catalyzes addition of these units to the outer chain utilizes α1→2-mannooligosaccharides as acceptors, but not those terminated with an α1→3-linked mannose unit (Karson & Ballou, 1978), it is possible that similar modification of the core side chains also regulates phosphorylation. Since the first α1→3-linked mannose added to the core oligosaccharide is a_5, its addition could occur at an early processing stage and thereby preclude subsequent phosphorylation at mannose A_3. Such a mechanism would provide a regulatory function for the 3-substitution of terminal α1→2-linked mannose in the mannoprotein.

A fourth α1→3-linked mannose is added to a small fraction of the *mnn2 mnn9* oligosaccharide, and since the acceptor for this addition has only terminal α1→3-linked mannose, we expect that this reaction is catalyzed by a unique transferase.

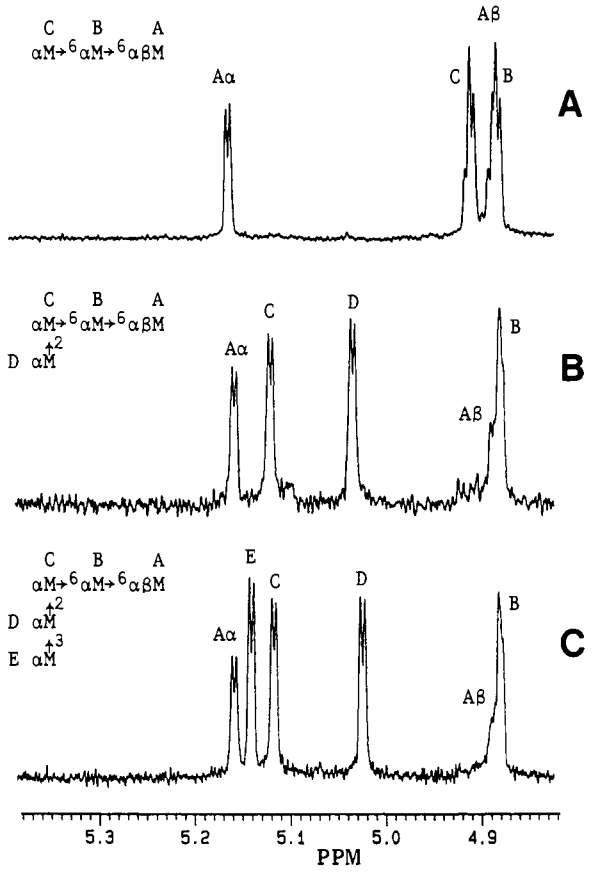

FIGURE 11: H-1 NMR spectra of peaks C–E from Figure 10. (A) Peak C of Figure 10B; (B) peak D of Figure 10B, which is identical with the mannotetraose fragment in peak D of Figure 10A (Ballou et al., 1989); (C) peak E of Figure 10B. Peaks D and E of Figure 10B come from the capped end of the outer chain, while C is from the central part of the outer chain. The location of the α1→3-linked mannose in the pentasaccharide fragment is based on methylation analysis and on the known specificity of the α1→3-transferase regulated by the MNN1 locus (Nakajima & Ballou, 1975). Note that the assignments for mannoses B and C in spectrum A are reversed from those in Cohen and Ballou (1980).

We have reported previously (Ballou et al., 1974) that *Saccharomyces chevalieri* makes αMan→3αMan→3αMan→-2αMan→2αMan→ side chains, and we described an enzyme activity that catalyzes addition of α1→3-mannosyl units to the acceptor αMan→3αMan→2αMan→2αMan→ to make the analogous structure (Nakajima & Ballou, 1975). In *S. cerevisiae*, this activity appears to be specific to the core because the acetolysis fragments from the outer chain do not show this modification (Nakajima & Ballou, 1975). Trimble and Atkinson (1986) did not localize this mannose unit in the $Man_{14}GlcNAc$ from yeast invertase, but we have made a tentative assignment to mannose d_3 in the $Man_{14}GlcNAc$ from the *mnn2 mnn9* mutant mannoprotein on the basis of the HOHAHA and ROESY NMR spectra. In the HOHAHA spectra, it was possible to correlate the deshielding of H-2 and H-3 protons of specific α1→2-linked mannose upon substitution at position 3, and the ROESY spectra allowed us to trace intra- and interresidue interconnectivities from H-1 of one mannose to H-3 of the mannose to which it is linked, and thence around the ring to H-2 and H-1 of this mannose. Although the differences in chemical shift on which the analysis was based were small, the conclusion appears justified.

Asparagine-linked oligosaccharides from the *mnn2 mnn10* strain contain an unbranched α1→6-linked outer chain that is terminated by an α1→2-linked mannose (Ballou et al., 1989), and this mannose also is substituted by an α1→3-linked mannose in the absence of the *mnn1* mutation. Some of the α1→3-linked mannose is also added to the core portion, and the splitting of the H-1 NMR signal for this mannose suggests that it may be distributed between the two available sites, mannoses A_4 and C_2.

The oligosaccharide structures we present here differ from those proposed by Trimble and Atkinson (1986) with regard to the position of attachment of the first α1→6-linked mannose during processing of the precursor $Man_8GlcNAc_2$ oligosaccharide. We have determined this to be position 6 of mannose A_2 in the *mnn2*, *mnn9*, and *mnn10* mutants (Hernandez et al., 1989a) whereas they have concluded the linkage is to position 6 of mannose C_1 in bakers' yeast invertase. Regardless, in both studies the addition of the α1→3-linked mannoses follows an ordered sequence at equivalent positions in both structures. Thus, the results are consistent even though the structures may be slightly different.

A biochemical role for these terminal α1→3-linked mannoses in yeast mannoproteins was suggested above, but their absence in the *mnn1* mutant and in at least one wild-type isolate leads to no apparently deleterious phenotype (Ballou & Raschke, 1974). On the other hand, the terminal α1→3-linked mannose in yeast mannoproteins is highly immunogenic in mammals (Ballou, 1970), and such linkages are notably absent in the N-linked oligosaccharides of higher eucaryotes (Kornfeld & Kornfeld, 1985). Thus, this structural modification may be a distinguishing feature of yeast and other fungi, and glycoproteins made in a *mnn1* mutant should be less immunogenic.

ACKNOWLEDGMENTS

Some preliminary studies on the *mnn9* oligosaccharides were carried out by Dr. P.-K. Tsai in this laboratory. We thank Aurora Trapane for help in isolating the mannoproteins and Nancy Northern for assistance in preparing the manuscript.

REFERENCES

Antalis, C., Fogel, S., & Ballou, C. E. (1973) *J. Biol. Chem. 248*, 4655–4659.

Ballou, C. E. (1970) *J. Biol. Chem. 245*, 1197–1203.

Ballou, C. E., & Raschke, W. C. (1974) *Science 184*, 127–134.

Ballou, C. E., Lipke, P. N., & Raschke, W. C. (1974) *J. Bacteriol. 117*, 461–467.

Ballou, L., Cohen, R. E., & Ballou, C. E. (1980) *J. Biol. Chem. 255*, 5986–5991.

Ballou, L., Alvarado, E., Tsai, P.-K., Dell, A., & Ballou, C. E. (1989) *J. Biol. Chem. 264*, 11857–11864.

Bax, A., & Davis, D. G. (1985) *J. Magn. Reson. 65*, 355–360.

Ciucanu, I., & Kerek, F. (1984) *Carbohydr. Res. 131*, 209–217.

Cohen, R. E., & Ballou, C. E. (1980) *Biochemistry 19*, 4345–4358.

Cohen, R. E., Zhang, W.-J., & Ballou, C. E. (1982) *J. Biol. Chem. 257*, 5730–5737.

Derome, A. E. (1987) *Modern NMR Techniques for Chemistry Research*, Pergamon Press, New York.

Hernandez, L. M., Ballou, L., Alvarado, E., Gillece-Castro, B. L., Burlingame, A. L., & Ballou, C. E. (1989a) *J. Biol. Chem. 264*, 11849–11856.

Hernandez, L. M., Ballou, L., Alvarado, E., Tsai, P.-K., & Ballou, C. E. (1989b) *J. Biol. Chem. 264*, 13648–13659.

Ichishima, E., Arai, M., Shigematsu, Y., Kumagai, H., & Sumida-Tanaka, R. (1981) *Biochim. Biophys. Acta 658*, 45–53.

Karson, E. M., & Ballou, C. E. (1987) *J. Biol. Chem. 253*, 6484–6492.

Kessler, H., Griesinger, C., Kerssebaum, R., Wagner, K., & Ernst, R. (1987) *J. Am. Chem. Soc. 109*, 607-609.
Kornfeld, R., & Kornfeld, S. (1985) *Annu. Rev. Biochem. 54*, 631-664.
Lee, Y. C., & Ballou, C. E. (1965) *Biochemistry 4*, 257-264.
Lindberg, B. (1972) *Methods Enzymol. 28*, 178-195.
Marion, D., & Wüthrich, K. (1983) *Biochem. Biophys. Res. Commun. 113*, 967-974.
Nakajima, T., & Ballou, C. E. (1974) *J. Biol. Chem. 249*, 7685-7694.
Nakajima, T., & Ballou, C. E. (1975) *Proc. Natl. Acad. Sci. U.S.A. 72*, 3912-3916.
Nakajima, T., Maitra, S. K., & Ballou, C. E. (1976) *J. Biol. Chem. 251*, 174-181.
Raschke, W. C., Kern, K. A., Antalis, C., & Ballou, C. E. (1973) *J. Biol. Chem. 248*, 4660-4666.
Saunier, B., Kilker, R. D., Jr., Tkacz, J. S., Quaroni, A., & Herscovics, A. (1982) *J. Biol. Chem. 257*, 14155-14161.
Trimble, R. B., & Atkinson, P. H. (1986) *J. Biol. Chem. 261*, 9815-9824.
Tsai, P.-K., Ballou, L., Esmon, B., Schekman, R., & Ballou, C. E. (1984a) *Proc. Natl. Acad. Sci. U.S.A. 81*, 6340-6343.
Tsai, P.-K., Frevert, J., & Ballou, C. E. (1984b) *J. Biol. Chem. 259*, 3805-3811.
Varki, A., & Kornfeld, S. (1980) *J. Biol. Chem. 255*, 10847-10858.
Vliegenthart, J. F. J., Dorland, L., & van Halbeek, H. (1983) *Adv. Carbohydr. Chem. Biochem. 41*, 209-374.

Effect of Oligosaccharides and Chloride on the Oligomeric Structures of External, Internal, and Deglycosylated Invertase†

Anthony V. Reddy, Robert MacColl, and Frank Maley*
Wadsworth Center for Laboratories and Research, New York State Department of Health, Empire State Plaza, Albany, New York 12201-0509

Received October 5, 1989; Revised Manuscript Received November 8, 1989

ABSTRACT: External invertase exists in an oligomeric equilibrium of dimer, tetramer, hexamer, and octamer, the concentrations of which vary with pH, time, and concentration of enzyme [Chu, F. K., Watorek, W., & Maley, F. (1983) *Arch. Biochem. Biophys. 223*, 543-555; Tammi, M., Ballou, L., Taylor, A., & Ballou, C. E. (1987) *J. Biol. Chem. 262*, 4395-4401]. To assess the influence of carbohydrate on this equilibrium, we investigated the self-association of external invertase (10 oligosaccharides per subunit), deglycosylated external invertase (2 oligosaccharides per subunit), and internal invertase (no carbohydrate) under various conditions. In addition, the effect of carbohydrate on the interaction of the subunits of these various invertases to form heterooligomers was studied. Chloride ion was found to promote subunit association in the various invertases irrespective of their glycosylation status. However, external invertase was less responsive to chloride ion relative to the internal and deglycosylated invertases. The higher oligomers of deglycosylated invertase were stable at 47 °C whereas those of external invertase dissociated rapidly into dimers, suggesting that the additional oligosaccharides in external invertase destabilize subunit interaction. Hybridization experiments with the various invertases showed that the dimers of internal invertase formed heterooligomers with either external or deglycosylated invertase. By contrast, the monomers of external and internal invertases formed their respective homodimers, but not heterodimers. These results suggest that the oligosaccharide content of invertase not only influences the extent of self-association but also affects heterooligomer formation.

The influence of oligosaccharides on the structure and function of glycoproteins has long been a subject of wide interest. Oligosaccharides are implicated in such functions as protein folding, stability, sorting, bioactivity, and protein–protein recognition. Invertase (EC 3.2.1.26, β-D-fructofuranoside fructohydrolase) from *Saccharomyces cerevisiae* is ideally suited to study the function of oligosaccharides since it exists as an external invertase with 50% (w/w) carbohydrate and an internal invertase with no carbohydrate. Both enzyme forms are derived from the SUC2 gene but from different start codons (Perlman & Halvorson, 1981; Carlson & Botstein, 1982). Because internal invertase does not contain a signal sequence, it cannot enter the endoplasmic reticulum and as a consequence is not glycosylated. By contrast, external invertase contains a signal sequence which directs it into the endoplasmic reticulum where it is glycoslyated to about 10 oligosaccharides per subunit (Trimble & Maley, 1977; Reddy et al., 1988), about 80% of which can be removed by endo-β-*N*-acetylglucosaminidase (Endo H)[1] (Tarentino et al., 1974). Eight of the oligosaccharides are from 8–14 mannoses in length while the remainder contain over 50 mannoses (Ziegler et al., 1988). Although oligosaccharides are not essential for enzyme activity, they protect the enzyme from proteases (Chu et al., 1978; Brown et al., 1979) and maintain external invertase in an oligomeric equilibrium of dimer, tetramer, hexamer, and octamer (Chu et al., 1983). More recently, it has been shown that freezing (Tammi et al., 1987) or the addition of poly-

† This work was supported in part by National Cancer Institute Grant CA 44355 from the U.S. Public Health Service, Department of Health and Human Services.
* To whom correspondence should be addressed.

[1] Abbreviations: buffer A, 0.05 M KH_2PO_4, pH 4.5; buffer B, 0.05 M sodium acetate, pH 5.5; CHES, 2-(*N*-cyclohexylamino)ethanesulfonic acid; Endo H, endo-β-*N*-acetylglucosaminidase H; GuHCl, guanidine hydrochloride; PEG, poly(ethylene glycol); RM-invertase, reductively methylated invertase.

0006-2960/90/0429-2482$02.50/0